

TITLE: NEUTRON INDUCED FISSION OF U ISOTOPES UP TO 100 MEV.

AUTHOR(S): Lestone, John P. and Gavron, Avigdur (P-17).

SUBMITTED TO: XII Meeting on Physics of Nuclear Fission  
September 27-30, 1993  
Institute of Physics & Power Engineering  
Obninsk, Kaluga Region, Russia

RECEIVED  
OCT 07 1993  
OSTI

By acceptance of this article, the publisher recognizes that the U.S. Government retains a nonexclusive, royalty free license to publish or reproduce the published form of this contribution, or to allow others to do so, for U.S. Government purposes.

The Los Alamos National Laboratory requests that the publisher identify this article as work performed under the auspices of the U.S. Department of Energy.

---

Los Alamos National Laboratory

Los Alamos, New Mexico 87545

FORM NO. 836 R4  
BT NO 2629 5-81

MASTER

## **Neutron Induced Fission of U Isotopes up to 100 MeV**

**J. P. Lestone and A. Gavron  
Los Alamos National Laboratory, Los Alamos, NM 87545, USA**

**August 30, 1993**

**For presentation at the  
XII Meeting on Physics of Nuclear Fission  
September 27-30, 1993  
Institute of Physics and Power Engineering  
Obninsk, Kaluga Region, Russia**

### **DISCLAIMER**

This report was prepared as an account of work sponsored by an agency of the United States Government. Neither the United States Government nor any agency thereof, nor any of their employees, makes any warranty, express or implied, or assumes any legal liability or responsibility for the accuracy, completeness, or usefulness of any information, apparatus, product, or process disclosed, or represents that its use would not infringe privately owned rights. Reference herein to any specific commercial product, process, or service by trade name, trademark, manufacturer, or otherwise does not necessarily constitute or imply its endorsement, recommendation, or favoring by the United States Government or any agency thereof. The views and opinions of authors expressed herein do not necessarily state or reflect those of the United States Government or any agency thereof.

# Neutron Induced Fission of U Isotopes up to 100 MeV

J. P. Lestone and A. Gavron

Los Alamos National Laboratory, Los Alamos, NM 87545, USA

## Abstract

We have developed a statistical model description of the neutron induced fission of U isotopes using densities of intrinsic states and spin cut off parameters obtained directly from appropriate Nilsson model single particle levels. The first chance fission cross sections are well reproduced when the rotational contributions to the nuclear level densities are taken into account. In order to fit the U(n,f) cross sections above the threshold of second chance fission, we need to: 1) assume that the triaxial level density enhancement is washed out at an excitation energy of  $\sim 7$  MeV above the triaxial barriers with a width of  $\sim 1$  MeV, implying a  $\gamma$  deformation for the first barriers of  $10^\circ < \gamma < 20^\circ$ ; and 2) include pre-equilibrium particle emission in the calculations. Above an incoming neutron kinetic energy of  $\sim 17$  MeV our statistical model U(n,f) cross sections increasingly overestimate the experimental data when so called "good" optical model potentials are used to calculate the compound nucleus formation cross sections. This is not surprising since at these high energies little data exists on the scattering of neutrons to help guide the choice of optical model parameters. A satisfactory reproduction of all the available U(n,f) cross sections above 17 MeV is obtained by a simple scaling of our calculated compound nucleus formation cross sections. This scaling factor falls from 1.0 at 17 MeV to 0.82 at 100 MeV.

## I. Introduction

The fission of actinides is extremely complex, depending on the heights and curvatures of saddle points, the density of single particle levels, collective level density enhancements, the properties of particle and  $\gamma$ -ray emission, compound nucleus formation cross sections and at moderate to high neutron energies on the properties of pre-equilibrium particle emission and possibly on the dynamics of the fission process. In this paper, we utilize elaborate cross section data available from the Weapons Neutron Research facility<sup>1,2</sup> (WNR) at Los Alamos, to examine what physics needs to be incorporated into the statistical model in order to fit U(n,f) cross sections up to an incoming neutron energy of 100 MeV.

We have analyzed fission cross sections,  $\sigma_f$ , for the six reactions  $^{232-236,238}\text{U}(n,f)$  at incoming neutron energies up to 100 MeV. Experimental  $^{233-236,238}\text{U}(n,f)$  cross sections for neutron energies of less than 3 MeV were obtained from the literature<sup>3</sup>, while, for the neutron energy range 3-100 MeV, we used cross sections recently measured at WNR<sup>1,2</sup>. For the  $^{232}\text{U}(n,f)$  reaction we used the first chance fission cross section measurements of ref 4. The statistical model analysis of the fission cross sections was performed with a version of the Hauser-Feshbach statistical model code PACE2<sup>5</sup>, modified to include the effects of the complex potential energy surface in actinides<sup>6</sup>. No changes were made to the way in which PACE2 calculates particle decay widths.

## II. The Model

Compound nucleus formation cross sections for the reactions  $n + ^{235}\text{U}$  and  $n + ^{238}\text{U}$  were determined using appropriate optical model potentials and ground state

shape parameters<sup>7</sup>, with the coupled channels code ECIS<sup>8</sup>. The optical model parameters of Haouat *et al.*<sup>9</sup>, which were obtained from analysis of low energy resonance data, neutron total cross section data, and neutron scattering data to 3.4 MeV, were modified slightly by Strottman and Mutschlechner<sup>10</sup> and Young<sup>7</sup> to cover the incident energy range to 100 MeV. This modification was made solely on the basis of neutron total cross section data<sup>11,12</sup>. Calculated cross sections for the reactions directly populating the ground state rotational band and low lying vibrational levels,  $\sigma_{\text{direct}}$ , were subtracted from calculated nuclear reaction cross sections,  $\sigma_{\text{R}}$ , to give compound nucleus formation cross sections  $\sigma_{\text{CN}}$ . Our calculated  $n + {}^{235}\text{U}$  and  $n + {}^{238}\text{U}$  compound nucleus formation cross sections differ by no more than 12% and 4% in the energy ranges of 0.5 - 4.0 MeV and 4 - 100 MeV, respectively. The averages of these two optical model calculations were used as the compound nucleus formation cross sections in the statistical model analysis of all the U(n,f) reactions presented in this paper. Our calculated  $n + \text{U}$  compound nucleus formation cross sections are shown in figure 1 by the solid line below 17 MeV and the dashed line. The solid line above 17 MeV will be described later.

For an equilibrated system, the fission decay widths were given by

$$\Gamma_f = \frac{1}{2\pi\rho_{\text{eq}}} \frac{N_1 N_2}{N_1 + N_2}$$

where  $\rho_{\text{eq}}$  is the level density of the fissioning system at the equilibrium deformation.  $N_1$ , and  $N_2$  are the number of available levels at the first barrier, and the mass asymmetric second barrier, respectively.

$$N = \int_0^{\epsilon} \rho(\epsilon) \left\{ 1 + e^{2\pi(\epsilon - B_f(J) + E_{\text{rot}}(J) - E) / \hbar\omega} \right\}^{-1} d\epsilon$$

where the height of the fission barrier,  $B_f(J)$ , and the rotational energy of the equilibrium configuration,  $E_{\text{rot}}(J)$ , are both functions of the angular momentum  $J$ ;  $\rho(\epsilon)$  is the level density as a function of the excitation energy  $\epsilon$  above the saddle point;  $\omega$  is the curvature of the saddle point; and  $E$  is the total excitation energy.  $E_{\text{rot}}(J)$  was calculated using the Rotating Finite Range Model<sup>13</sup> (RFRM). The angular momentum dependence of the barrier heights was given by

$$B_f(J) = B \times \frac{B^{\text{RFRM}}(A, Z, J)}{B^{\text{RFRM}}(A, Z, 0)}$$

where  $B^{\text{RFRM}}(A, Z, J)$  are RFRM fission barriers and  $B$  is the height of the barrier at  $J = 0$ .

The nuclear level density for a deformed axially symmetric nucleus is<sup>14</sup>

$$\rho_{\text{ax}}(E, J) = \frac{(2J + 1) \Omega(E - E_{\text{rot}}(J))}{(8\pi)^{1/2} \sigma_{\parallel}(E - E_{\text{rot}}(J))}$$

and for a triaxial nucleus

$$\rho_{\text{tri}}(\mathbf{E}, \mathbf{J}) \approx (2J + 1) \Omega(\mathbf{E} - \mathbf{E}_{\text{rot}}(\mathbf{J}))$$

where  $\Omega$  is the density of intrinsic states, and  $\sigma_{\parallel}$  is the spin cutoff parameter (parallel to the symmetry axis). Note that  $\rho_{\text{tri}}$  is enhanced relative to  $\rho_{\text{ax}}$  by a factor of  $(8\pi)^{1/2} \sigma_{\parallel}$ . For the mass asymmetric second barrier the level density was multiplied by an additional factor of two because of the reflection asymmetry<sup>14</sup>. For the statistical model analysis presented here, both  $\Omega$  and  $\sigma_{\parallel}$  were obtained directly from appropriate Nilsson model<sup>15</sup> single particle levels, using codes written by P. Möller<sup>16</sup> and S. M. Grimes<sup>17</sup>. The parameters chosen to specify the shapes of the equilibrium deformation and saddle points<sup>18</sup> are shown in table I. Even though the first saddle is  $\gamma$  deformed, we still calculate the density of intrinsic states at the first barrier assuming an axially symmetric shape. We feel this is justified since the difference between an axially symmetric and triaxial level density is dominated by the triaxial level density enhancement factor of  $(8\pi)^{1/2} \sigma_{\parallel}$  and is relatively insensitive to any dependence of  $\Omega$  on the  $\gamma$  deformation.

### III. Analysis

Table II shows the  $J = 0$  barrier heights needed to reproduce the  $^{232-236,238}\text{U}(n,f)$  cross sections up to the threshold for second chance fission, assuming a triaxial first barrier height  $E_A$  and a mass asymmetric second barrier height  $E_B$ . The barrier curvatures were assumed to be the same as in ref 19. To reproduce the odd- $\text{U}(n,f)$  cross sections below  $E_n \sim 1$  MeV it was necessary to use the larger of  $\Omega = \Omega_{\text{Nilsson}}$  or  $\Omega \sim 7 \text{ MeV}^{-1}$ , for the density of intrinsic states at the equilibrium deformation. This gives a nearly constant total level density for the odd mass ground states of  $\sim 60$  levels per MeV below an excitation energy of  $\sim 1$  MeV. Above 1 MeV the total level density increases in an exponential fashion. Such behavior at low energies is consistent with level densities used by other authors<sup>20,21</sup>. The solid curves in figure 2 show our calculated fission cross sections using the barrier heights given in table II. The  $^{238}\text{U}$  barrier heights given in table II were determined by a study of the systematics of our  $^{233-237,239}\text{U}$  barrier heights and an analysis of measured  $^{238}\text{U}(\gamma,f)$  fission probabilities<sup>22,23</sup>.

With the set of barriers shown in table II, we can extend our calculations of the  $^{233-236,238}\text{U}(n,f)$  cross sections up to the thresholds of third and higher chance fission, respectively. The dashed and dotted lines in figure 2 show such calculations, with and without the inclusion of pre-equilibrium particle emission, calculated using the geometry dependent hybrid model<sup>24</sup>. These calculations significantly overestimate the fission cross sections above an incoming neutron energy of  $E_n \sim 7$  MeV. We postulate that this overestimation of the  $\text{U}(n,f)$  cross sections is due to the washing out of the triaxial level density enhancement factor  $(8\pi)^{1/2} \sigma_{\parallel}$ . Hansen and Jensen<sup>25</sup> have used a one-shell  $\text{SU}(3)$  model to study the washing out of collective level density enhancements in excited nuclei. They suggest the following parameterization of the triaxial level density enhancement :

$$R_t = 1 + f_t + f_t (8\pi)^{1/2} \sigma_{\parallel}(\mathbf{E} - \mathbf{E}_{\text{rot}}(\mathbf{J}))$$

$$f_t = \left\{ 1 + e^{-(\mathbf{E} - \mathbf{E}_{\text{rot}}(\mathbf{J}) - E_t)/\delta_t} \right\}^{-1}$$

$\delta_t$  determines the width of the transition from  $R_t = (8\pi)^{1/2} \sigma_{||}$  at  $E - E_{\text{ToI}}(J) \ll \epsilon_t$  to  $R_t = 1$  at  $E - E_{\text{ToI}}(J) \gg \epsilon_t$ . Hansen and Jensen found no apparent difference between the level densities of axially symmetric and triaxial nuclei above an excitation energy of 20 MeV, thus implying  $\epsilon_t < 20$  MeV.

All the following statistical model calculations include the effects of pre-equilibrium emission. Table III shows the triaxial level density enhancement washing out parameters which give the best fits to the  $^{233-236,238}\text{U}(n,f)$  second chance fission cross sections. The  $^{238}\text{U}$  triaxial level density enhancement washing out parameters were estimated using the  $^{238}\text{U}(n,f)$  third chance fission cross sections. The solid curves in figure 2 show  $U(n,f)$  cross sections calculated up to 20 MeV using these washing out parameters. Figure 3 compares measured  $^{235,238}\text{U}(n,2n)$  and  $^{235,238}\text{U}(n,3n)$  cross sections with calculations using these same barriers and washing out parameters. The good agreement with these experimental data (which complement the fission cross section data) gives us increased confidence in the model we have presented. The rise in the even- $U(n,f)$  cross sections at the threshold of second chance fission is due to the competition between  $\gamma$  emission and fission of even- $U$  nuclei at an excitation energy approximately equal to the height of the fission barriers. The strength of the  $\gamma$  emission which gives the best fit to the rise in the even- $U(n,f)$  second chance fission cross sections is also in good agreement with known  $\gamma$  widths at the neutron binding energy of actinides. Once above the threshold of even- $U(n,f)$  second chance fission the cross sections are again determined by the competition between neutron emission and fission, and the  $\gamma$  emission only plays a minor role.

Hansen and Jensen<sup>25</sup> state, that it is plausible that

$$\epsilon_t = \frac{A h^2}{\gamma_t} (\omega_x + \omega_y)^2 \quad \text{and} \quad \delta_t = \frac{h^2}{\nu_t} (\omega_x - \omega_y)^2$$

with  $\gamma_t = 14 \pm 3$  MeV and  $\nu_t = 1.2 \pm 0.5$  MeV.  $\omega_x$  and  $\omega_y$  are the frequencies used to define the potential energy of the individual nucleons in the x and y directions. The z direction is along the scission (fission) axis. We stress that these values for  $\gamma_t$  and  $\nu_t$  are suggestions obtained from the study of the washing out of the axially symmetric level density enhancement factor (which occurs at a much higher excitation energy) using only symmetry and plausibility arguments. Using these relationships between the triaxial level density enhancement washing out parameters and the frequencies  $\omega_x$  and  $\omega_y$ , the  $\epsilon_t$  values shown in table III imply  $\gamma$  deformations for the first saddle points of U isotopes of  $11 \pm 2^\circ$ , while the corresponding  $\delta_t$  values imply a  $\gamma$  deformation of  $18 \pm 6^\circ$ . These estimates are in agreement with modified oscillator model predictions of the  $\gamma$  deformation of the first saddle points of Uranium nuclei<sup>30</sup>.

To extend our calculations of the  $^{233-236,238}\text{U}(n,f)$  cross sections to a neutron energy of 100 MeV it was necessary to estimate the fission barriers of U isotopes down to mass 230. This was done with a simple linear least squares fit to our  $^{233-237,240}\text{U}$  barrier heights. For all isotopes not listed in table III the triaxial level density enhancement washing out parameters were assumed to be  $\epsilon_t = 7.2$  MeV and  $\delta_t = 0.82$  MeV. In order to model the relatively small amount of fission of non-U isotopes produced by charged particle emission, La and Th fission barriers were obtained by extrapolating barriers given

in ref 19. Above  $\sim 17$  MeV our statistical model  $U(n,f)$  cross sections increasingly over estimate the experimental data when so called "good" optical model potentials are used to calculate the compound nucleus formation cross sections. This is shown by the dashed curves in figure 4. At first one might be tempted to believe that this discrepancy is associated with a dynamical hindrance of the fission process due to a finite value of the nuclear viscosity, since a hindrance of the fission process will lead to a decrease in the fission probability. Evidence of a dynamical hindrance of the fission process has been found in many studies of heavy ion induced fission<sup>31</sup>. To test this possibility we have simulated the effect of infinite nuclear dissipation at moderate to high excitation energy by completely suppressing all fission above an excitation energy of 30 MeV. This leads to a reduction of 10% in our calculated 100 MeV  $^{238}\text{U}(n,f)$  cross section but leaves our 100 MeV  $^{233}\text{U}(n,f)$  cross section essentially unchanged. Both the size of this effect and its dependence on target mass are inconsistent with the experimental data. Within an accuracy of 5% the relative discrepancy between our model calculations and the experimental  $U(n,f)$  cross sections is independent of target mass. A satisfactory reproduction of all the available  $U(n,f)$  cross sections above 17 MeV can be obtained by a simple scaling of our calculated compound nucleus formation cross sections. This scaling factor falls from 1.0 at 17 MeV to 0.82 at 100 MeV. Figure 5 shows the  $n + \text{U}$  compound nucleus formation cross section scaling factor as a function of neutron energy, which leads to the best overall reproduction of the  $U(n,f)$  data. A scaling of our calculated compound nucleus formation cross sections is not unreasonable since at these high energies little data exists on the scattering of neutrons to help guide the choice of optical model parameters. The solid curves above 17 MeV in figures 1 and 4 show our modified  $n + \text{U}$  compound nucleus formation cross sections and the corresponding calculated  $U(n,f)$  cross sections.

#### IV. Conclusions

We have developed a statistical model description of 0.5 - 100 MeV neutron induced fission of U isotopes using densities of intrinsic states and spin cut off parameters obtained directly from Nilsson model single particle levels. In order to satisfactorily reproduce the available data we: 1) wash out the triaxial level density enhancements; 2) include the effects of pre-equilibrium particle emission; and 3) modify our optical model compound nucleus formation cross sections above a neutron energy of 17 MeV. No useful information about the effect of nuclear dissipation on the  $U(n,f)$  reaction can be obtained by a study of only the fission cross section data. Pre-scission neutron data from the  $^{238}\text{U}(n,f)$  reaction obtained at WNR are presently being analyzed and should provide a detailed picture of the effects of nuclear dissipation on  $U(n,f)$  reactions.

We would like to thank M. Blann for providing us with his geometry dependent hybrid pre equilibrium emission code; and P. Young for his calculation of  $n + \text{U}$  reaction and direction reaction cross sections.

## References

1. P. W. Lisowski *et al.*, in Proc. 50 Years with Nuclear Fission, Washington, D.C. and Gaithersburg, Maryland, 25-28 April 1989, pg. 443, American Nuclear Society, Inc. La Grange Park 1989.
2. P. W. Lisowski *et al.*, in Proc. Nuclear Data for Science and Technology, Jülich, Germany, 13-17 May 1991, pg. 752, Springer-Verlag Berlin Heidelberg, 1992.
3. V. McLane *et al.*, "Neutron Cross Sections, Vol. 2," Academic Press, Inc. San Diego, 1988.
4. B. I. Fursov *et al.*, *At. Energ.* **61**, 383 (1986).
5. A. Gavron, *Phys. Rev. C* **21**, 230 (1980).
6. A. Gavron *et al.*, *Phys. Rev. C* **13**, 2374 (1976).
7. P. Young, Los Alamos National Laboratory, private communication.
8. J. Raynal, "Optical Model and Coupled-Channel Calculations in Nuclear Physics," International Atomic Energy Agency Report, SMR-9/8 (1970).
9. Haouat *et al.*, *Nucl. Sci. Eng.* **81**, 491 (1982).
10. D. D. Strottman and A. D. Mutschlechner, Los Alamos National Laboratory Progress Report, LA-11972-PR (1990).
11. W. P. Poenitz *et al.*, *Nucl. Sci. Eng.* **78**, 333 (1981).
12. P. W. Lisowski *et al.*, in Proc. Symposium on Neutron Cross-Sections from 10 to 50 MeV, Upton, New York, 12-14 May 1980, Vol. I, pg. 301, National Nuclear Data Center, Brookhaven National Laboratory, Upton, New York, BNL-NCS-51245.
13. A. J. Sierk, *Phys. Rev. C* **33**, 2039 (1986).
14. S. Bjornholm *et al.*, in Proc. of the Third International Atomic Energy Symposium on Physics and Chemistry of Fission, Rochester, 1973, Vol. I, pg. 367, International Atomic Energy Agency, Vienna, 1974.
15. S. G. Nilsson *et al.*, *Nucl. Phys. A* **131**, 1 (1969).
16. P. Möller, Los Alamos National Laboratory, private communication.
17. S. M. Grimes, Ohio University, private communication.
18. P. Möller, in Proc. of the International Symposium on Physics and Chemistry of Fission, Jülich, 1979, Vol. I, pg. 283, International Atomic Energy Agency, Vienna, 1980.
19. S. Bjornholm and J. E. Lynn, *Rev. Mod. Phys.* **52**, 725 (1980).
20. B. B. Back *et al.*, *Phys. Rev. C* **10**, 1948 (1974).
21. A. V. Ignatyuk and V. M. Maslov, to be published.
22. P. A. Dickey and P. Axel, *Phys. Rev. Lett.* **35**, 501 (1975).
23. J. T. Caldwell *et al.*, Los Alamos National Laboratory Report, LAUR 76-1615 (1976).
24. M. Blann and H. K. Vonach, *Phys. Rev. C* **28**, 1475 (1983).
25. G. Hansen and A. S. Jensen, *Nucl. Phys. A* **406**, 236 (1983).
26. J. Frehaut *et al.*, *Nucl. Sci. Eng.* **74**, 29 (1980).
27. L. R. Veesser and E. D. Arthur, *Neutron Physics and Nuclear Data*, OECD, Harwell, 1054 (1978).
28. N. V. Kornilov *et al.*, VANI Series on Nuclear Constants [in Russian], *TSNIAtominform, M.*, 1982, No. 1 (45), pg. 33.
29. J. Frehaut and G. Mosinski, in *Neutron Physics* [Russian transl.], *TSNIAtominform, M.*, 1976, Part 4, pg. 303.
30. S. E. Larsson and G. Leander, in Proc. of the Third International Atomic Energy Symposium on Physics and Chemistry of Fission, Rochester, 1973, Vol. I, pg. 177, International Atomic Energy Agency, Vienna, 1974.
31. D. Hilscher and H. Rossner, *Ann. Phys. Fr.* **17**, 471 (1992).

## Tables

Table I. Parameters used to define the shapes of the equilibrium deformation and the saddle points of U isotopes.

	$\epsilon_2$	$\epsilon_3$	$\epsilon_4$
equilibrium deformation	+ 0.20	0.00	- 0.06
triaxial first barrier	+ 0.45	0.00	+ 0.04
mass asymmetric second barrier	+ 0.88	- 0.18	0.00

Table II. Heights of the triaxial first barrier  $E_A$  and the mass asymmetric second barrier  $E_B$  (at  $J = 0$ ) needed to reproduce the  $^{232-236,238}\text{U}(n,f)$  cross sections up to the threshold for second chance fission.

Isotope	$E_A$ (MeV)	$E_B$ (MeV)
$^{233}\text{U}$	6.0	5.7
$^{234}\text{U}$	5.9	5.7
$^{235}\text{U}$	5.9	5.7
$^{236}\text{U}$	6.0	5.7
$^{237}\text{U}$	5.9	5.9
$^{238}\text{U}$	6.0	5.8
$^{239}\text{U}$	6.0	5.8

Table III. Triaxial level density enhancement washing out parameters which give the best fit to the  $^{233-236,238}\text{U}(n,f)$  cross sections above the threshold of second chance fission.

Isotope	$\epsilon_1$ (MeV)	$\delta_1$ (MeV)
$^{234}\text{U}$	7.7	0.6
$^{235}\text{U}$	7.8	0.7
$^{236}\text{U}$	8.0	0.6
$^{237}\text{U}$	5.5	1.1
$^{238}\text{U}$	7.5	0.7
$^{239}\text{U}$	6.5	1.2

## Figure captions

Figure 1. The  $n + U$  compound nucleus formation cross sections. The solid line below 17 MeV and the dashed line show our calculated cross sections obtained using the optical model parameters discussed in the text. The solid line above 17 MeV shows the compound nucleus formation cross sections which lead to the best over-all reproduction of the available  $U(n,f)$  data.

Figure 2. Comparison between experimental  $U(n,f)$  cross sections, circles, and statistical model calculations. The solid curves are calculated  $U(n,f)$  cross sections using the barriers and triaxial level density enhancement washing out parameters presented in tables II and III with the inclusion of pre-equilibrium emission. The dashed curves are calculations with no washing out of the triaxial level density enhancements. The dotted curves are the same as the dashed without the inclusion of pre-equilibrium emission.

Figure 3. Experimental  $^{235,238}U(n,2n)$  and  $^{235,238}U(n,3n)$  cross sections (circles - ref 26; squares - ref 27; up triangles - ref 28; and down triangles - ref 30). The curves show the corresponding calculations using the barrier heights and triaxial level density enhancement washing out parameters presented in tables II and III; and the geometry dependent hybrid pre-equilibrium emission model.

Figure 4. Comparison between experimental  $U(n,f)$  cross sections in the energy range 0.5 - 100 MeV with our statistical model calculations. The solid line below 17 MeV and the dashed line show our calculated  $U(n,f)$  cross sections using the compound nucleus formation cross sections obtained using the optical model parameters discussed in the text. The solid line above 17 MeV shows the fission cross sections obtained when the compound nucleus formation cross sections are adjusted to give the best over-all fit to the available  $U(n,f)$  data.

Figure 5. The  $n + U$  compound nucleus formation cross section scaling factor as a function of neutron energy which leads to the best over-all reproduction of the  $U(n,f)$  data.

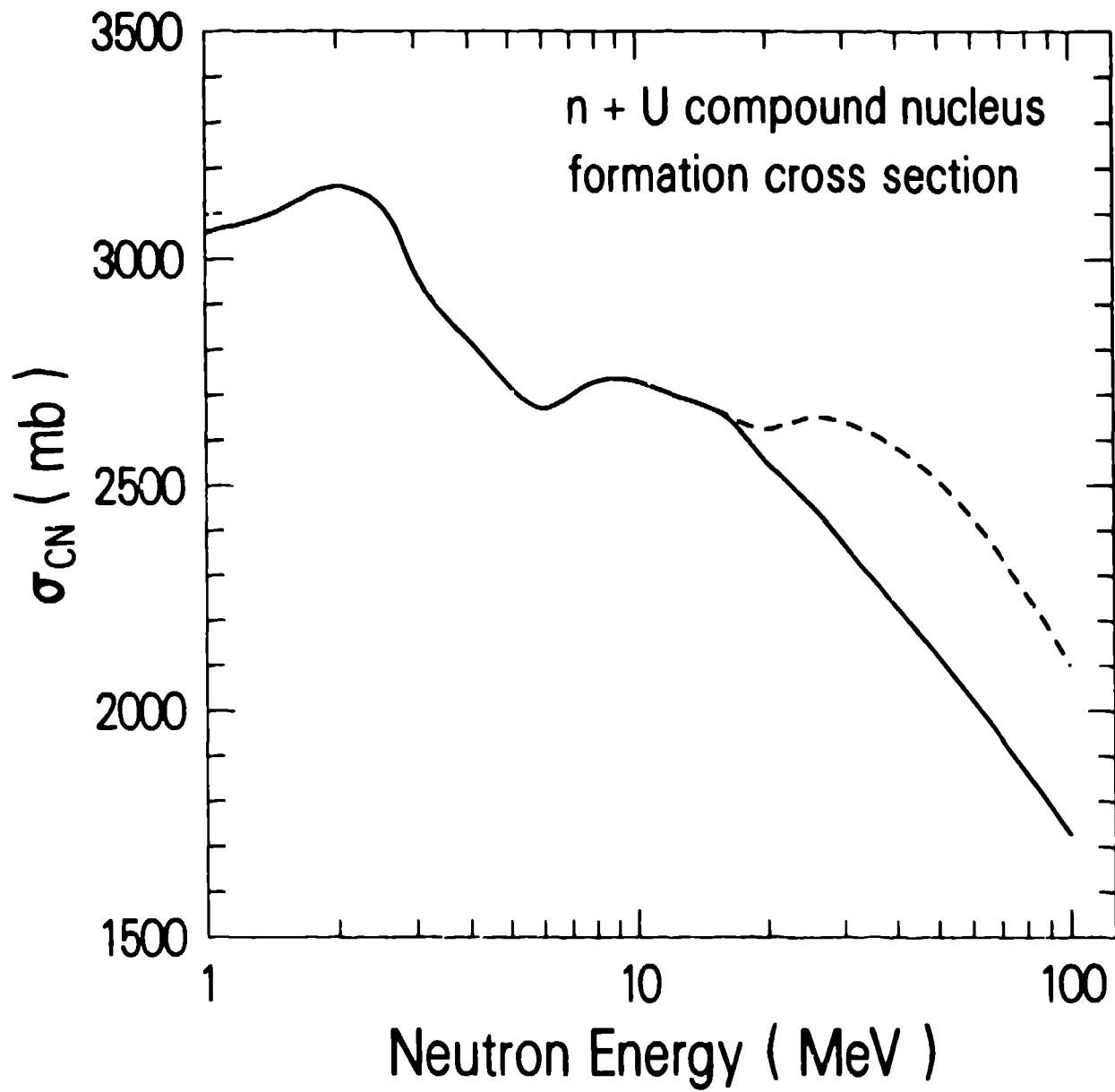


Figure 1.

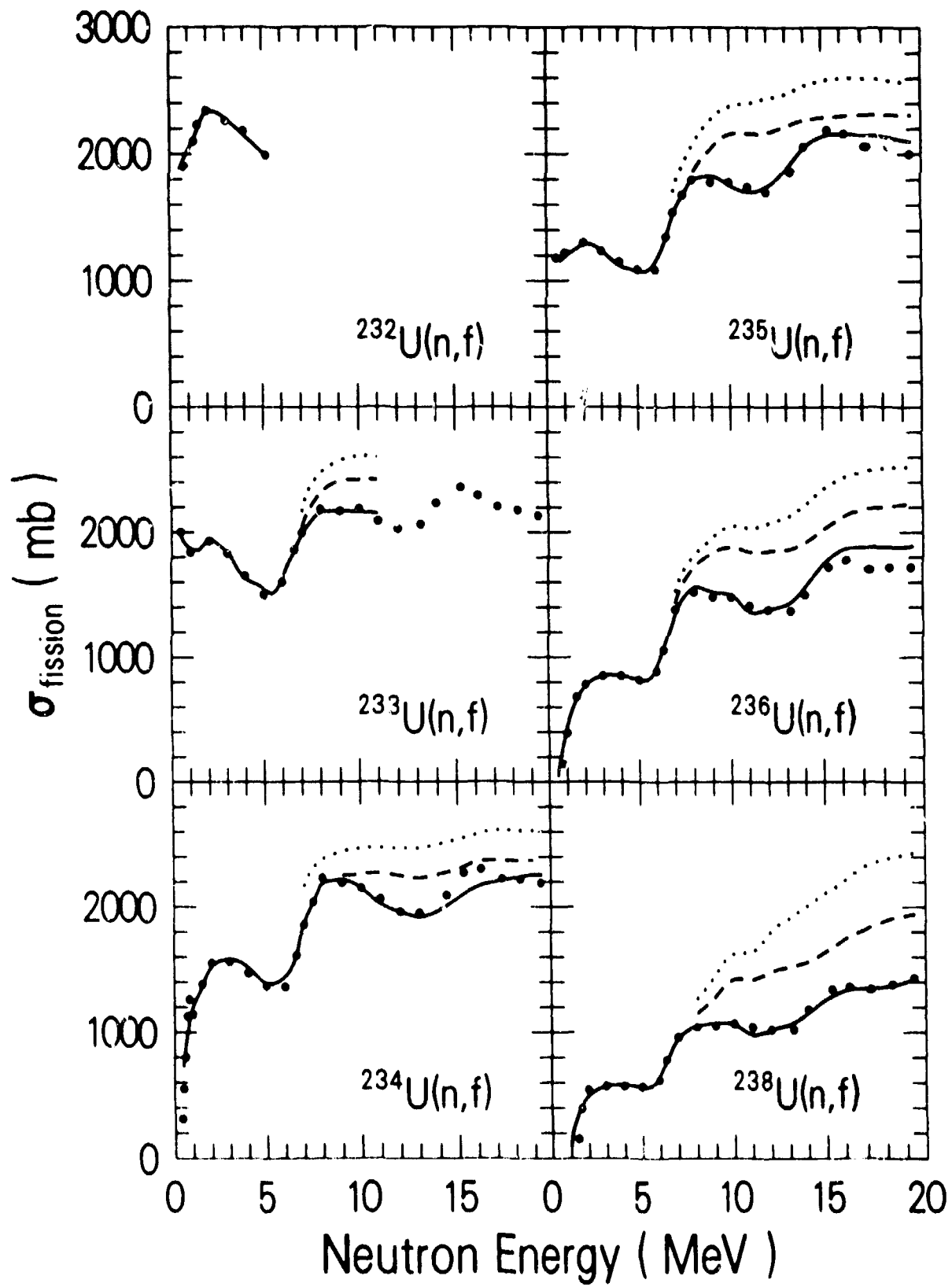


Figure 2.

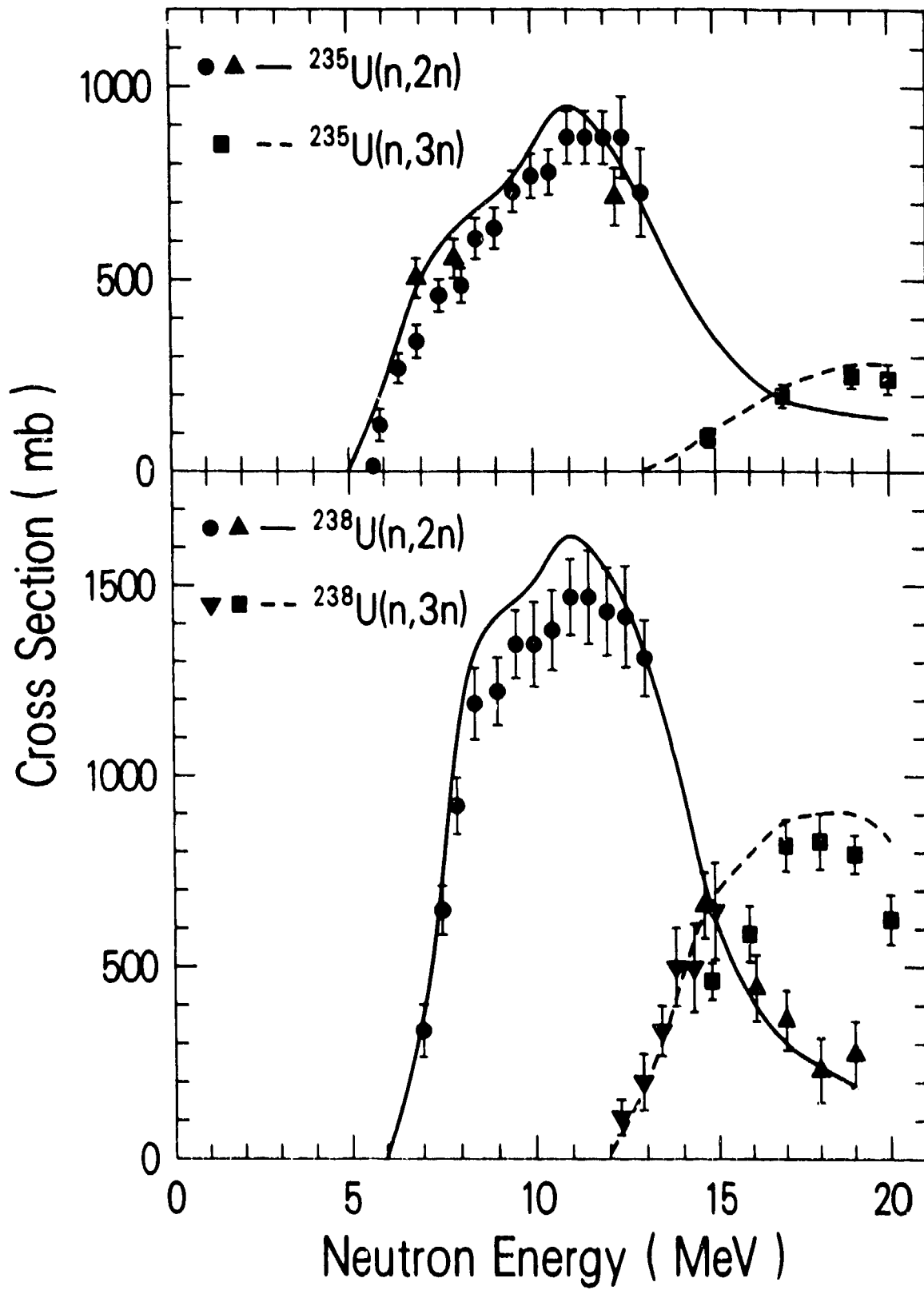


Figure 3.

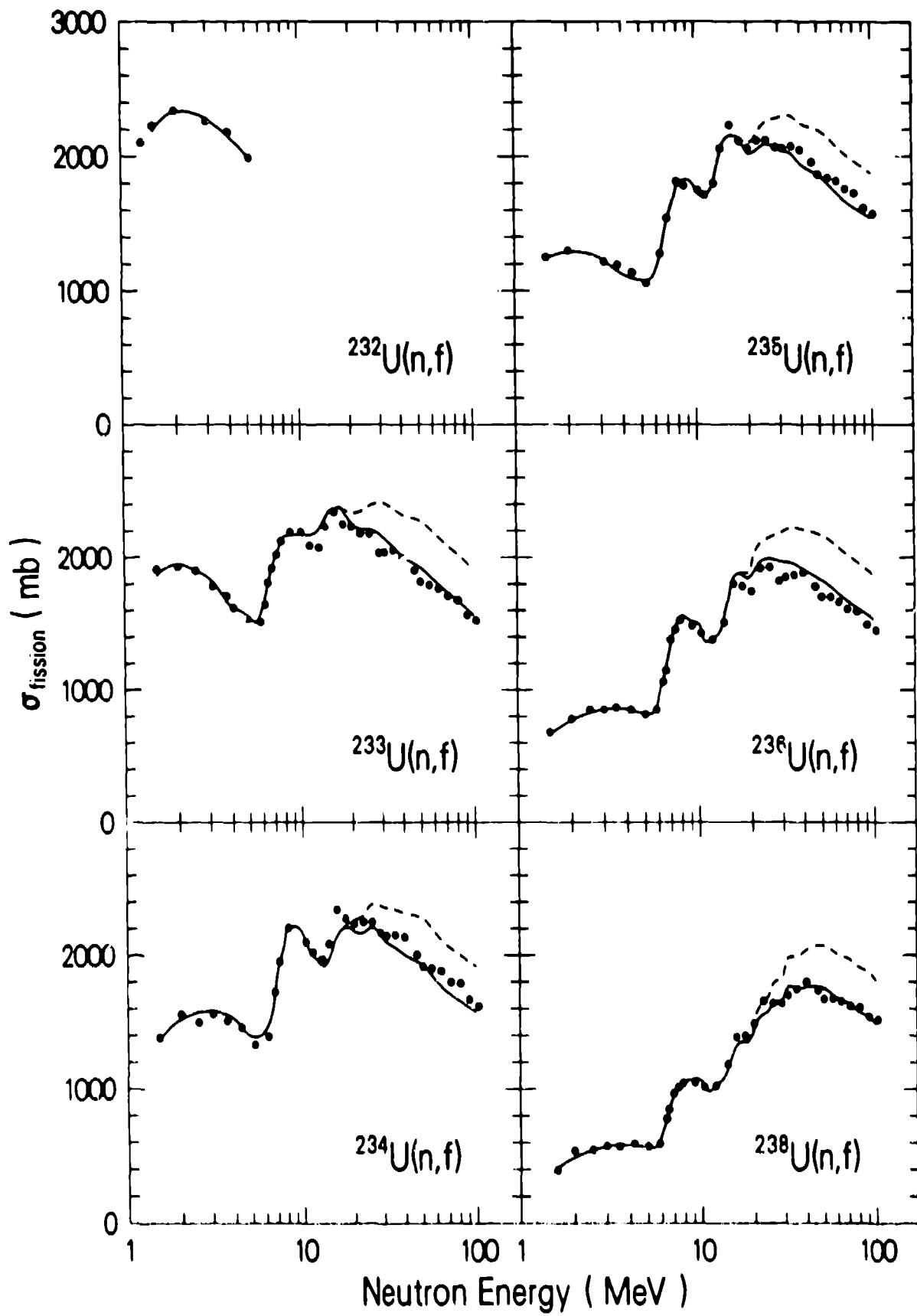


Figure 4.

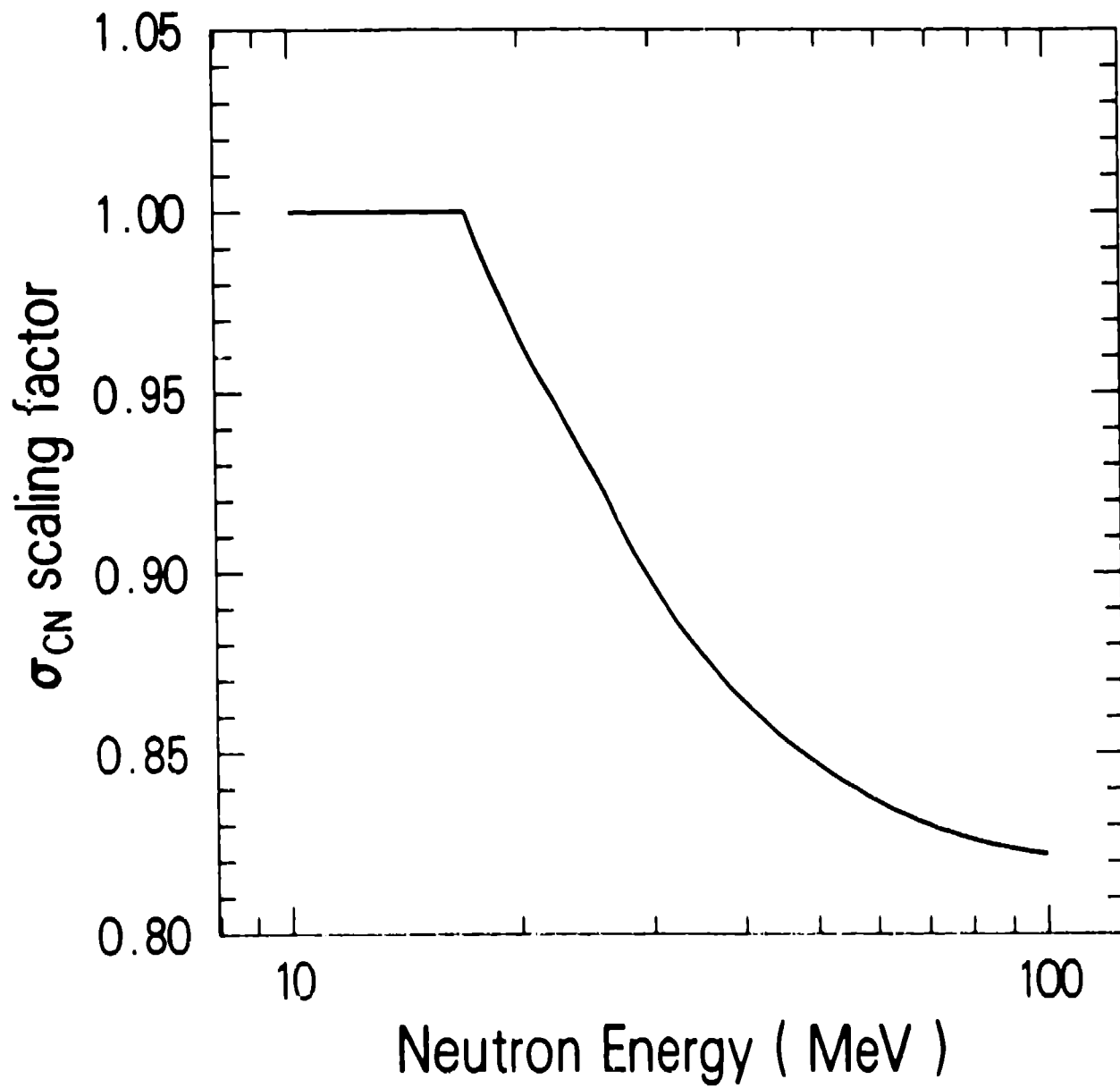


Figure 5.